Broadband Dielectric Investigation of Amorphous Poly(methyl methacrylate)/Poly(ethylene oxide) Blends

Xing Jin, Shihai Zhang, and James Runt*

Department of Materials Science and Engineering, and Materials Research Institute, The Pennsylvania State University, University Park, Pennsylvania 16802

Received April 13, 2004; Revised Manuscript Received August 4, 2004

ABSTRACT: The segmental and local dynamics of amorphous blends of poly(methyl methacrylate) and poly(ethylene oxide) (PMMA/PEO) were investigated using dielectric relaxation spectroscopy. The derivative of the dielectric permittivity facilitates the observation of the cooperative segmental relaxation (α_b) in blends with low PEO content, which is mostly masked in ϵ'' spectra. For blends aged at room temperature, a DSC endotherm gradually develops near the expected PEO T_m and shifts to higher temperatures with increasing aging time. However, X-ray diffraction from PEO crystals is not observed, indicating that the glassy blends undergo physical aging at room temperature. A relaxation appears in the blends between the PMMA and PEO local relaxations, which we propose is associated with regions of PEO partial order.

1. Introduction

In the past decade nanoscale dynamic heterogeneities have been identified in globally miscible polymer blends, in which the components have a relatively large difference in mobility ($\Delta T_g \geq 50$ °C) and do not exhibit strong intermolecular associations. This heterogeneity has been explained using the concepts of concentration fluctuations,[1] intrinsic mobility differences,[2] and self-concentration effects arising from chain connectivity.[3] Even more complex relaxation behavior may occur in melt-miscible polymer blends containing a crystallizable component, the classic examples of which are blends of poly(methyl methacrylate) (PMMA) with poly(ethylene oxide) (PEO) and poly(vinylidene fluoride) (PVDF).

It was initially reported that relatively high molecular weight PMMA/PEO blends have a small negative Flory−Huggins interaction parameter, χ, and it was proposed that these mixtures are miscible across the entire composition range in the melt as well as in the amorphous portion of semicrystalline blends.[4] In keeping with this interpretation, a lower critical solution temperature (LCST) of ∼350 °C was predicted for atactic PMMA/PEO blends having M_w (g/mol) of 1.3×10^5 and 2.0×10^4, respectively.[5] However, a variety of later experimental findings are at variance with these reports. Solid-state nuclear magnetic resonance (NMR) has been used to investigate the heterogeneity of PMMA/PEO blends (with $M_w = 9 \times 10^4$ and 2×10^5 g/mol in refs 6 and 7 and 3×10^6 and 5×10^6 g/mol in ref 8) containing 10% and 18% PEO at room temperature. A heterogeneous domain size of between ∼2 and ∼50 nm was estimated from proton spin−lattice relaxation times in the rotating frame ($T_{1\rho}(^1H)$) and the laboratory reference frame ($T_1(^1H)$), respectively.[6] On the basis of the chemical shift and bandwidth of ^{129}Xe absorbed in these blends, the heterogeneity was estimated to be on a scale of ∼40 nm.[7] In another study on a 80/20 PMMA/PEO blend ($M_w = 1.17 \times 10^5$ and 2×10^4 g/mol), the blend composition was calculated from the NMR $T_{1\rho}(^1H)$ decay and free induction decay at room temperature.[9] The difference between the calculated composition from NMR and the known bulk composition suggested the presence of ∼5 wt % phase-separated PEO in addition to a mixed amorphous phase. These authors postulated that the phase-separated PEO arose from constrained and crystalline units, but no PEO crystallinity was detected by DSC.

Infrared dichroism and birefringence measurements, combined with rheometry, demonstrated that the two components have distinct relaxation times and temperature dependences in PMMA-rich blends.[10] On the basis of measurements of χ (derived from small-angle neutron scattering experiments), it was concluded that an upper critical solution temperature (UCST) occurs near ∼320−350 K for amorphous PMMA/PEO blends with $M_w \sim 10^5$ g/mol (both components) and PEO volume fractions of 0.1−0.27.[11] These authors argued that their results differ from those reported earlier[4] since the earlier studies did not take into consideration the effect of deuteration on the measured χ's.

In an extension of our previous studies of the segmental and local dynamics of globally miscible polymer blends and solutions, we use broadband dielectric spectroscopy to probe the local environments of amorphous blends of atactic PMMA and PEO. In particular, we focus on the effects of room temperature aging on the observed heterogeneity.

2. Experimental Section

2.1. Materials. The PMMA used in the present study was purchased from Aldrich Chemical Co. Given that PMMA tacticity can play a role in its miscibility with PEO,[12,13] the tacticity of the PMMA used in our experiments was determined by ^1H NMR (300 MHz, $CDCl_3$ as the solvent). It was found to consist of $rr/rm/mm = 34\%/45\%/11\%$, where r and m represent racemic and meso diads, respectively. Therefore, this polymer can be considered to be atactic (*a*-PMMA). The relative M_w and M_n were found to be 9.5×10^4 and 3.9×10^4 g/mol, respectively, as determined from gel permeation chromatography (GPC), using tetrahydrofuran as the mobile phase and nearly monodisperse polystyrene standards.

The PEO used in our experiments was purchased from Polysciences. M_w and M_n were determined from GPC to be 2.2×10^5 and 5.4×10^4 g/mol, respectively, using dimethylforma-

* To whom correspondence should be addressed: e-mail runt@matse.psu.edu; phone 1-814-8632749; fax 1-814-8650016.

10.1021/ma049281b CCC: $27.50
Published on Web 09/25/2004

mide containing 0.05 M LiBr as the mobile phase. Calibration was performed using PEO standards (M_w/M_n < 1.1) from Polymer Standards Service.

Neat PMMA and PEO powders were pressed at 190 and 100 °C, respectively, for several minutes. The pressed films were placed into a vacuum oven preheated at 130 and 100 °C, respectively. After heating in a vacuum for 45 min, the heater was turned off, and the samples were maintained under vacuum for 1 day until the oven slowly cooled to room temperature. PMMA/PEO blends were prepared from $CHCl_3$ solutions. Mixed solutions were stirred for >6 h. After solution-casting onto Al foil, samples were placed in a hood at room temperature for >12 h and then heated in a vacuum with the temperature gradually increased to avoid bubble formation. After heating at the final temperature of 130 °C for < 1 h, the heater was turned off, and samples were maintained under vacuum until the oven slowly cooled to room temperature. The blend samples are denoted as M*x* hereafter, where *x* is the wt % PMMA.

2.2. Techniques. 2.2.1. Dielectric Relaxation Spectroscopy (DRS). DRS spectra were collected using a Novocontrol Concept 40 broadband dielectric spectrometer. Temperature control was accomplished using a Novocontrol Quatro Cryosystem. Experiments were run in the frequency domain (0.01 Hz−10 MHz), using 7.5 °C increments. The minimum stabilization time after the temperature reached a given value (±0.3 °C) was 1 min. Specimens ∼0.6 mm thick were sandwiched between two electrodes and had diameters a little larger than that of the upper electrode (20 mm).

Two different temperature profiles were applied: (a) dielectric measurements were performed on cooling from 190 to −140 °C, and (b) samples were held at 190 °C for 10 min, then cooled to 130 °C and held for 30 min, and then aged at 25 °C for 1 day. The cooling rate from 130 to 25 °C was ∼8 °C/min. Measurements were then conducted on heating from −140 to 190 °C. Samples were always maintained under an N_2 blanket during in situ thermal processing and measurement. The samples with the above two thermal histories are denoted as "unaged" and "aged", respectively.

DRS Data Processing. The dc conduction losses prevalent at low frequencies can mask the intrinsic relaxations of the samples, especially at higher temperatures. To circumvent this difficulty, we make use of an "ohmic conduction-free" dielectric loss, ϵ''_{der}:[14]

$$\epsilon''_{der} = -\frac{\pi}{2}\frac{\partial \epsilon'(f)}{\partial \ln f} \quad (1)$$

where ϵ' is the real part of the dielectric permittivity and f is the frequency. To perform the differentiation, we used a numerical technique based on a low pass quadratic least-squares filter.[15] A series of model calculations were conducted and ϵ''_{der} and ϵ'' shown to exhibit the same peak frequencies, provided the relaxations are relatively broad (as they are in the present case), and the relaxation strength of the derivative spectrum is a good approximation to that of ϵ''.[16] We have also previously demonstrated the reliability of this procedure on a similar blend system.[17] The peak temperatures (T_{max}) of relaxations at individual experimental frequencies were read from contour plots of ϵ''_{der} in a map of temperature and frequency.

2.2.2. Differential Scanning Calorimetry (DSC). All DSC measurements were performed on a TA Instruments Q-100 apparatus. The temperature and transition enthalpy were calibrated using an indium standard. Sample weights were ∼10 mg.

To measure T_g, samples were first heated to 190 °C, held for 10 min, and cooled to −140 °C at ∼10 °C/min; then T_g was acquired on heating at 10 °C/min. In other cases, samples were directly cooled from room temperature to −140 °C at ∼10 °C/min and then heated at 10 °C/min; the thermograms from the subsequent heating step are reported below.

2.2.3. Wide-Angle X-ray Diffraction (WAXD). WAXD experiments were conducted on a Scintag instrument using Cu Kα radiation ($\lambda = 0.154$ nm) at 35 kV and 30 mA. Samples were scanned continuously at 1 or 2°/min using an increment of 0.02°. A silicon zero-background substrate was used to support the samples in all cases.

3. Results and Discussion

3.1. DRS. PMMA exhibits a segmental α relaxation and a local β process, and the latter is much stronger than the former in dielectric spectra of *a*- and syndiotactic PMMA.[18] PEO exhibits at least three relaxations below its melting point.[18] For semicrystalline PEO, the higher temperature relaxation is associated with the crystalline phase. The β_{PEO} process originates from cooperative motions of disordered interlamellar amorphous segments. The lower temperature γ_{PEO} relaxation has been assigned to local twisting in the main chains. In addition, we recently reported the observation of a relaxation between the β_{PEO} and γ_{PEO} processes, which we denoted as γ'_{PEO}.[19] The available evidence suggested that this process arises from the motion of PEO segments in the transition region between ordered crystalline lamellae and disordered interlamellar amorphous segments. The unusual local character of the γ'_{PEO} process was rationalized by analogy to the fast process or primitive segmental relaxation in nanoconfined glass-forming systems.

Figure 1 displays the 3D DRS spectrum of an unaged M90 blend. Visualizing the dielectric loss data in ϵ''_{der} form permits the cooperative segmental relaxation of the blend, α_b, to be clearly observed (although it is mostly masked in the ϵ'' spectrum[20]), as well as the local PMMA β and PEO γ relaxations and a merged $\alpha_b + \beta_{PMMA}$ process (denoted as $\alpha\beta$; see also Figure 2).

Figure 3 displays the 3D DRS spectrum of an M80 blend aged 1 day at 25 °C (then measured at gradually increasing temperatures). A relaxation (labeled β') appears between the PMMA β and PEO γ relaxations and also becomes evident in the spectra of the other blends after aging (the frequency−temperature ($f-T$) locations are plotted in Figure 4). There is also a hint of this process in the spectra of unaged blends at nearly the same $f-T$ location as the aged mixtures, but overlap with the high-frequency side of the PMMA β process (along with its low magnitude) makes it difficult to resolve, and so $f-T$ locations are not provided for unaged blends in Figure 4. Note that β_{PEO} is not observed in the blends, and data for this neat PEO process are plotted in Figure 4 only to facilitate later discussion. The proposed origin of the β' process will be discussed below, after presentation of DSC and WAXD results.

For all of the blends investigated here, the PEO γ relaxation is observed, and its $f-T$ location remains essentially invariant with blend composition but appears at somewhat higher frequencies than the γ process of neat PEO (see Figures 2 and 4). This suggests weaker local constraints for the γ relaxation in amorphous blends than in semicrystalline PEO. In Figure 5, the α_b and $\alpha\beta$ processes are observed to shift to lower temperatures with increasing PEO content, as anticipated for a transition associated with a mixed noncrystalline phase. For unaged blends, the significant loss at low frequencies (arising at least partially from electrode polarization) obscures a significant portion of the M85 α_b relaxation and completely masks the α_b process of the M80 blend (Figure 2). For aged blends, the loss at low frequencies is so significant that the α_b

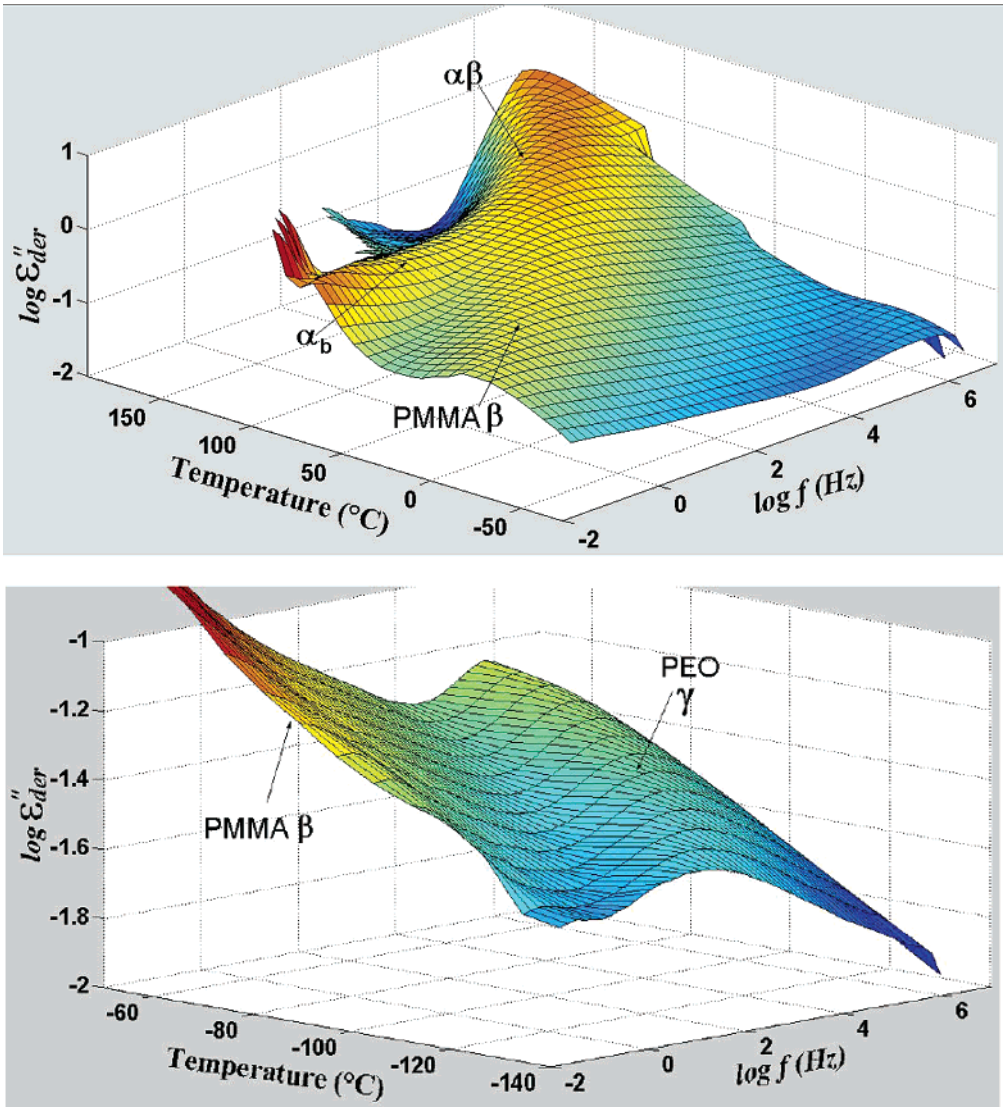

Figure 1. 3D DRS spectrum of the unaged M90 blend: (a, top) relatively high temperatures; (b, bottom) lower temperatures.

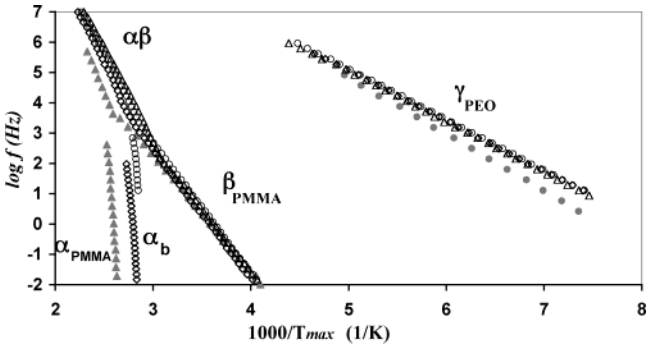

Figure 2. Peak frequency vs T^{-1} for the DRS relaxations of unaged blends compared with those of the neat components. Symbols: (1) components (filled symbols): triangles, PMMA; circles, semicrystalline PEO from ref 19. (2) Blends (unfilled symbols): diamonds, M90; circles, M85; triangles, M80.

relaxation cannot be resolved even in the spectra of M85 (Figure 4).

3.2. DSC. In Figure 6 it is seen that blends with ≥80% PMMA exhibit a single T_g, which moves to lower temperatures with increasing PEO content, suggesting miscibility. However, the thermogram of the M70 blend exhibits what appears to be two T_gs, including a lower T_g near −30 °C. Similar behavior has been reported previously for PMMA/PEO blends having 25−50% PEO.[21] For all blends, the breadths of the T_g intervals are much broader than that of neat PMMA, and upon aging at room temperature an endotherm appears (close to the melting temperature (T_m) of PEO crystallites), which shifts to higher temperatures with increasing aging time (Figure 7). As demonstrated later, this endotherm does not originate from PEO crystal melting, but from physical aging at room temperature of the glassy blends.

Multiple T_gs were not observed for either the M90 or M80 blends up to an aging time of almost 6 months, demonstrating that blends with PMMA composition ≥80 wt % are in the one-phase region of the phase diagram, at least for polymers of the molecular weight used in the present study. Therefore, it is not suitable to argue that phase separation is the origin of the nanoheterogeneities in this composition range, as detected previously by solid-state NMR experiments. The M70 blend, however, appears to be in the two-phase region of its blend phase diagram, consistent with the existence of a UCST whose phase boundary passes through room temperature at a composition between 20 and 30% PEO.

Considering that T_g has been proposed to correspond to a relaxation time of 100 s,[22] the DSC onset T_g is reached by extrapolating the $f-T$ locations of the DRS

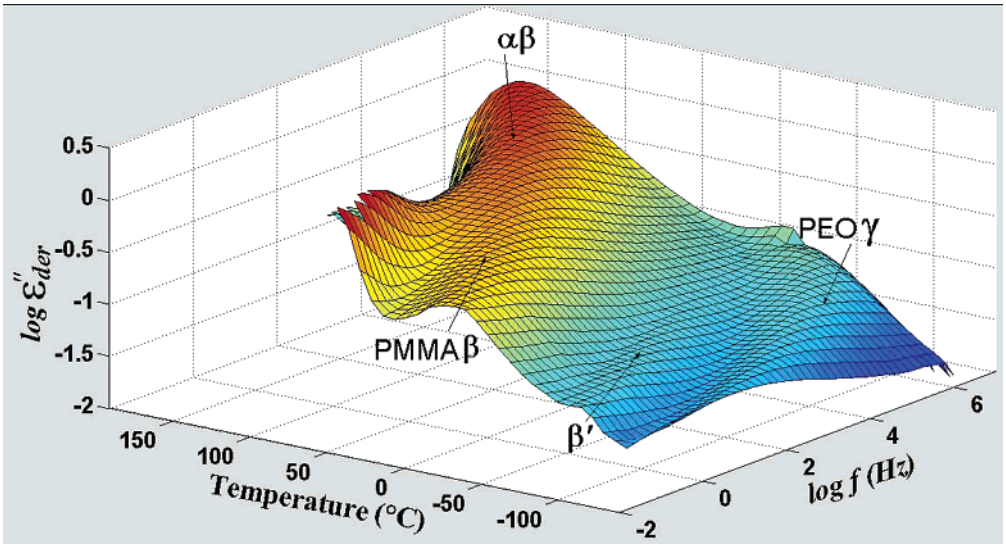

Figure 3. 3D DRS spectrum of M80 aged for 1 day at room temperature.

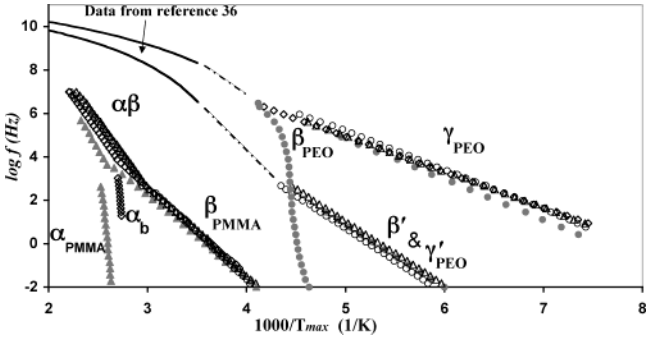

Figure 4. Peak frequency vs T^{-1} for DRS relaxations of the aged blends compared with those of the neat components. NMR data from ref 36 have also been added to the plot for comparison purposes. Symbols: (1) components (filled symbols): triangles, PMMA; circles, PEO, from ref 19. (2) Aged blends (unfilled symbols): diamonds, M90; circles, M85; triangles, M80. Solid lines are data for the PEO segmental relaxation from ref 36. From top to bottom: neat PEO, PMMA/PEO blend having 20% PEO. Dashed lines are only to guide the eyes.

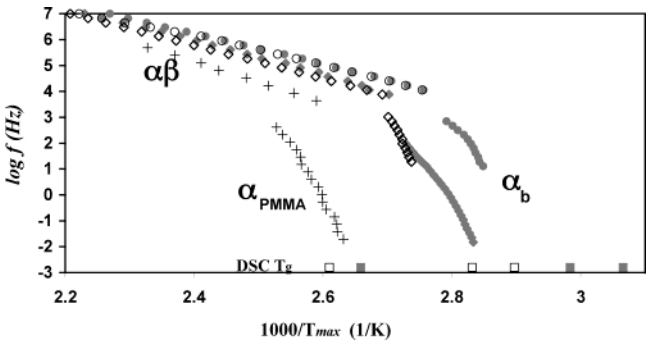

Figure 5. Peak frequency vs T^{-1} for the DRS α and $\alpha\beta$ processes and comparison of the α relaxation with the DSC T_g. Symbols: (1) DRS data: crosses, PMMA. Blends (unaged samples = filled symbols; aged samples = unfilled symbols): diamonds, M90; circles, M85. (2) DSC T_g data, assuming that T_g corresponds to a relaxation time of 100 s (at the bottom of the plot, from left to right: PMMA, M90, M85): filled squares, onset DSC T_g; unfilled squares, midpoint DSC T_g.

α process of neat PMMA (Figure 5), similar to our previous observations for other neat polymers and certain polymer blends.[17,23] For the M90 and M85 blends, however, the temperature at which the dielectric

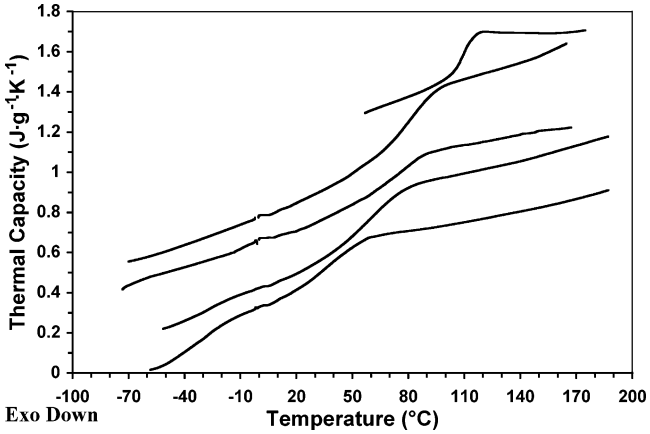

Figure 6. DSC thermograms from about −60 to 160 °C. From top to bottom: PMMA, M90, M85, M80, M70.

α_b relaxation time reaches 100 s is instead closer to the DSC midpoint T_g.

3.3. WAXD. PMMA/PEO blends with high PEO content exhibit two strong crystalline X-ray reflections at the same 2θ (∼20° and ∼24° for Cu Kα radiation) as neat PEO.[24] However, these reflections are absent in the diffraction pattern of M80 blends aged for 1 and 11 days—only an amorphous halo is observed (Figure 8), despite the existence of a DSC endotherm near T_m(PEO) for aged blends. Even for a phase-separated M70 blend aged at room temperature for 6 months, the diffraction pattern exhibits only an amorphous halo (Figure 8).

Since no cold crystallization occurs on heating above room temperature, the observed endotherms clearly do not originate from the melting of PEO crystallites. However, this behavior is completely consistent with the expectations of physical aging below the blend T_g. Physical aging of polymer glasses has been studied widely,[25] but aging of glassy polymer blends has been investigated less frequently.[26,27] In an early investigation of a 50/50 wt % polystyrene−poly(vinyl methyl ether) (PS/PVME) blend, aged at temperatures near the blend onset T_g, evidence suggests that PVME ages independently of PS and is responsible for essentially all of the aging effects measured.[27]

3.4. Origin of the *β′* Process. First, the possibility that trace water is the origin of the β' process in blends can be ruled out. No such relaxation of water was

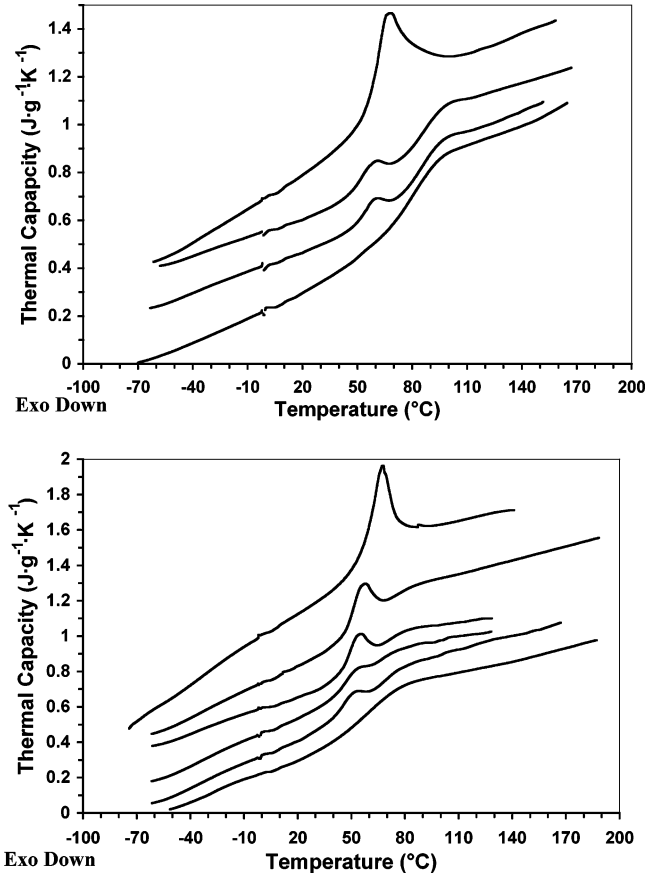

Figure 7. DSC thermograms illustrating the influence of room temperature aging. The aging times at room temperature for the blends, from top to bottom: (a, top) M90: 5.5 months, 2 days, 1 day, unaged; (b, bottom) M80: 5.7 months, 7 days, 2 days, 1 day, 9 h, unaged.

observed in the spectra of our neat PMMA, which was subjected to the same high-temperature processing, storage, and experimental conditions as the blend samples. In addition, for PEO samples containing very small to modest water contents, the water relaxation closest to the β' process is observed at still lower temperatures and higher frequencies.[19,28]

What occurs during the aging process that leads to significant enhancement of the strength of the β' relaxation? First, it is particularly intriguing to note that the $f-T$ locations of the β' relaxation are essentially the same as those we observed previously for the relaxation of neat *semicrystalline* PEO we referred to as γ' (Figure 4). The latter process was assigned to a segmental relaxation, exhibiting reduced cooperativity and involving segments in the transition regions between the ordered crystal and disordered noncrystalline segments.[19] Clearly, such transition regions do not exist per se in the aged blends, since no 3D crystallinity is observed, as noted above. However, we propose that the β' process is associated with regions of PEO partial order, formed to a very small extent during initial sample preparation but to a greater degree during physical aging. We also propose that this is connected to recent models for the early stages of structure development during polymer crystallization that have invoked the formation of a partially ordered mesophase[29] or "baby nuclei/smectic pearls"[30] as a precursor to crystal formation.

A dielectric transition with similar characteristics has been reported previously in amorphous blends of PMMA and crystallizable poly(vinylidene fluoride) (PVDF).[31] The formation of PEO and PVDF partial order in their blends with PMMA is not unexpected considering that there are principally kinetic restrictions to either of these polymers crystallizing from these blends.[32] Finally, recall that the β' process of the blends (and the γ' process of neat PEO) occurs at temperatures *below* that of the PEO cooperative segmental process. This has many similarities to observations for thermotropic main-chain liquid crystalline polymers, for which the segmental relaxation in the liquid crystalline (mesomorphic) glassy state occurs at a *lower* temperature than in the isotropic amorphous glass (see ref 33 and references therein).

Further support for the formation of PEO partial order on aging comes from several studies on amorphous PEO/PMMA blends with relatively low PEO content. A ^{1}H NMR investigation of blends of hydrogenated PEO and deuterated PMMA demonstrated that, for blends with PEO $\leq$ 0.5 wt %, the maximum in the spin−lattice relaxation rate was below the blend T_g, which suggested that PEO chains dispersed in the rigid PMMA matrix remain mobile even below the blend T_g.[34] Recently, it was found that the diffusion of diethyl ether in a PEO/PMMA blend containing 20% PEO is rapid at room temperature, with diffusion constants more typical for elastomers than for glasses.[35] From the temperature dependence of $T_{1\rho}(^{13}C)$ and $T_1(^{13}C)$ of PEO in PEO/PMMA blends with 10−18% PEO, it was estimated that

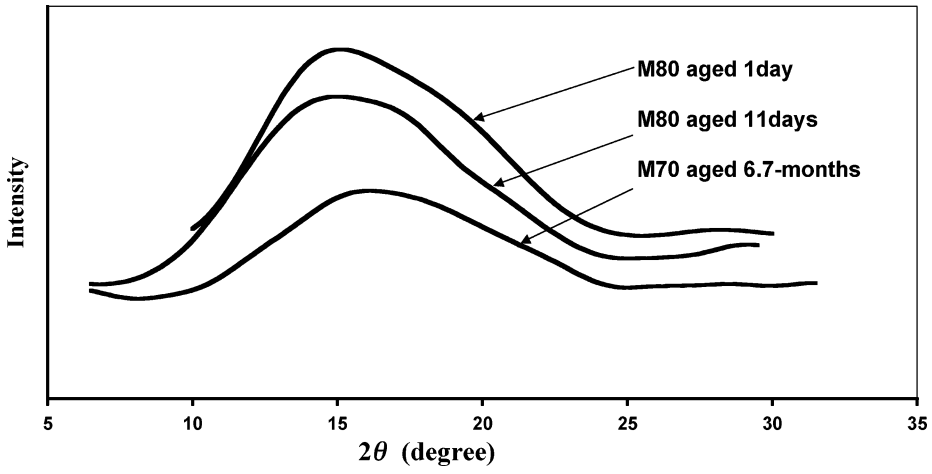

Figure 8. WAXD results for selected aged blends.

the PEO relaxation at 27 °C was only slightly increased: from 1.7×10^{-10} s for neat PEO to 4.2×10^{-10} s.[6] The above evidence supports the view that in amorphous PMMA/PEO blends at least a portion of the PEO segments retains sufficient mobility to permit organization into regions of partial order at room temperature.

Very recently, a ^{2}H NMR study revealed that near the blend T_g the *segmental* relaxation of PEO is 12 orders of magnitude faster than that of PMMA in PMMA/PEO blends (M_w (g/mol): $1.06 \times 10^5/1.25 \times 10^5$) containing ≤30% PEO.[36] The dynamics of PEO segments are only somewhat slower in the blends than in the neat state (by about 2 orders of magnitude at the lowest temperatures investigated), and PEO segmental relaxation times were found to be essentially the same for blends with 10, 20, and 30 wt % PEO. The PEO *segmental* relaxation frequencies from ref 36 for neat PEO (semicrystalline) and an amorphous 20% PEO/PMMA blend are plotted together with our data in Figure 4. To a first-order approximation, these values can be connected with the dielectric peak frequencies of the merged $\beta + \gamma$ relaxation of neat crystalline PEO and the β' process of the 20% PEO blend. This lends further support to the assignment of the β' process as a PEO *segmental* process.

4. Summary

Visualizing the dielectric loss data in ϵ''_{der} form permits the observation of the cooperative segmental relaxation of amorphous PMMA/PEO blends, α_b, which are mostly masked in ϵ'' spectra. DSC data demonstrate that blends with ≥80% PMMA exhibit a single T_g, while the M70 blend exhibits what appears to be two T_gs. For all blends, the breadths of the T_g intervals are much broader than that of neat PMMA. Upon aging the blends at room temperature, an endotherm appears close to the PEO T_m and shifts to higher temperatures with increasing aging time. However, X-ray diffraction from PEO crystallites is absent. These findings are readily explained by physical aging of the glassy blends at room temperature.

A process denoted as β' was observed in the dielectric spectra of the amorphous blends. We present evidence from this and other studies that it is associated with regions of PEO partial order, formed to a rather small extent during initial sample preparation, but to a greater degree during physical aging.

Acknowledgment. The authors express their appreciation to the National Science Foundation, Polymers Program (DMR-0211056), for support of this research and the NSF-MRI program for support of the dielectric instrumentation (DMR-0079432). We also thank K. Li and M. Kanchanasopa for assistance with the ^{1}H NMR and WAXD experiments, respectively.

References and Notes

(1) Kamath, S.; Colby, R. H.; Kumar, S. K.; Karatasos, K.; Floudas, G.; Fytas, G.; Roovers, J. E. L. *J. Chem. Phys.* **1999**, *111*, 6121.
(2) Chung, G. C.; Kornfield, J. A.; Smith, S. D. *Macromolecules* **1994**, *27*, 964.
(3) Lodge, T. P.; McLeish, T. C. B. *Macromolecules* **2000**, *33*, 5278.
(4) Ito, H.; Russell, T. P.; Wignall, G. D. *Macromolecules* **1987**, *20*, 2213.
(5) Cimmino, S.; Martuscelli, E.; Silvestre, C. *Polymer* **1989**, *30*, 393.
(6) Schantz, S. *Macromolecules* **1997**, *30*, 1419.
(7) Schantz, S.; Veeman, W. S. *J. Polym. Sci., Polym. Phys.* **1997**, *35*, 2681.
(8) Straka, J.; Schmidt, P.; Dybal, J.; Schneider, B.; Spevacek, J. *Polymer* **1995**, *36*, 1147.
(9) Parizel, N.; Laupretre, F.; Monnerie, L. *Polymer* **1997**, *38*, 3719.
(10) Zawada, J. A.; Ylitalo, C. M.; Fuller, G. G.; Colby, R. H.; Long, T. E. *Macromolecules* **1992**, *25*, 2896.
(11) Hopkinson, I.; Kiff, F. T.; Richards, R. W.; King, S. M.; Farren, T. *Polymer* **1995**, *36*, 3523.
(12) Silvestre, C.; Cimmino, S.; Martuscelli, E.; Karasz, F. E.; MacKnight, W. J. *Polymer* **1987**, *28*, 1190.
(13) Marco, C.; Fatou, J. G.; Gomez, M. A.; Tanaka, H.; Tonelli, A. E. *Macromolecules* **1990**, *23*, 2183.
(14) Steeman, P. A. M.; van Turnhout, J. *Macromolecules* **1994**, *27*, 5421.
(15) Gory, P. A. *Anal. Chem.* **1990**, *62*, 570.
(16) Wübbenhorst, M.; van Turnhout, J. *J. Non-Cryst. Solids* **2002**, *305*, 40.
(17) Jin, X.; Zhang, S. H.; Runt, J. *Macromolecules* **2003**, *36*, 8033.
(18) McCrum, N. G.; Read, B. E.; Williams, G. *Anelastic and Dielectric Effects in Polymer Solids;* Dover Publications: New York, 1967.
(19) Jin, X.; Zhang, S. H.; Runt, J. *Polymer* **2002**, *43*, 6247.
(20) Dionísio, M.; Fernandes, A. C.; Mano, J. F.; Correia, N. T.; Sousa, R. C. *Macromolecules* **2000**, *33*, 1002.
(21) Li, X.; Hsu, S. L. *J. Polym. Sci., Polym. Phys.* **1984**, *22*, 1331.
(22) Angell, C. A. *J. Non-Cryst. Solids* **1991**, *131*−*133*, 13.
(23) Jin, X.; Zhang, S. H.; Horvath, J. R.; Runt, J. *J. Phys. Chem. B* **2004**, *108*, 7681.
(24) Lisowski, M. S.; Liu, Q.; Cho, J.; Runt, J.; Yeh, F.; Hsiao, B. S. *Macromolecules* **2000**, *33*, 4842.
(25) Hutchinson, J. M. *Prog. Polym. Sci.* **1995**, *20*, 703.
(26) Vernel, J.; Rychwalski, R. W.; Pelisek, V.; Saha, P.; Schmidt, M.; Maurer, F. H. J. *Thermochim. Acta* **1999**, *342*, 115.
(27) Cowie, J. M. G.; Ferguson, R. *Macromolecules* **1989**, *22*, 2312.
(28) Jin, X.; Zhang, S. H.; Runt, J. Manuscript in preparation.
(29) Grasruck, M.; Strobl, G. *Macromolecules* **2003**, *36*, 86.
(30) Muthukumar, M. *Philos. Trans. R. Soc.* **2003**, *A361*, 539.
(31) Ando, Y.; Yoon, D. Y. *Polym. J.* **1992**, *24*, 1329.
(32) Runt, J. In *Polymer Blends: Formulation and Performance*; Paul, D. R., Bucknall, C., Eds.; Wiley: New York, 2000; Vol. 1, Chapter 6.
(33) Garcia-Bernabea, A.; Diaz Calleja, R.; Sanchisa, M. J.; del Campob, A.; Bellob, A.; Perez, E. *Polymer* **2004**, *45*, 1533.
(34) Lartigue, C.; Guillermo, A.; Cohen-Addad, J. P. *J. Polym. Sci., Polym. Phys.* **1997**, *35*, 1095.
(35) Lin, G.; Zhang, J.; Cai, H.; Jones, A. A. *J. Phys. Chem. B* **2003**, *107*, 6179.
(36) Lutz, T. R.; He, Y.; Ediger, M. D.; Cao, H.; Lin, G.; Jones, A. A. *Macromolecules* **2003**, *36*, 1724.

MA049281B